Dilution and clustering of Fe in the rutile phases of TiO_2 and SnO_2

A. I. Rykov,[1,2,*] K. Nomura,[1] J. Sakuma,[1] C. Barrero,[1] Y. Yoda,[3] and T. Mitsui[4]
[1]*Department of Applied Chemistry, The University of Tokyo, Hongo 7-3-1, Bunkyo-ku, Tokyo 113-8656, Japan*
[2]*Synchrotron Radiation Methods No 9 Laboratory of ISSCM SB RAS, Siberian Synchrotron Radiation Center, Budker Institute of Nuclear Physics, Lavrent'eva 11, Novosibirsk, 630090, Russia*
[3]*Japan Synchrotron Radiation Research Institute, Sayo, Hyogo 679-5198, Japan*
[4]*Japan Atomic Energy Research Institute, Kouto 1-1-1, Mikazuki, Sayo, Hyogo 679-5198, Japan*
(Received 23 November 2006; revised manuscript received 21 May 2007; published 25 January 2008)

Dilute magnetic semiconductors of Fe-doped SnO_2 and TiO_2 with the structure of rutile were prepared in forms of powder and thin films using the techniques of sol gel and pulsed-laser deposition. We present the results of measurement of vibrational density of states of Fe impurity dopants in these oxides and demonstrate the cases of dilution and clustering. The oxygen pressure during the film deposition was varied between 10^{-1} and 10^{-8} Torr. In TiO_2 films made at 10^{-1} Torr, Fe is diluted, however, in films made at 10^{-8} Torr Fe is clustered. The case of true Fe dilution in SnO_2 is also shown. In spite of larger mass defect for Fe in SnO_2 than that for Fe in TiO_2 the dilute Fe species probe the phonon states in SnO_2 more faithfully than in TiO_2. This result is understood in terms of the combined effect of mass defect and nearest-neighbor force-constant changes. The impurity modes are more pronounced in TiO_2 than in SnO_2 due to ca. 10% difference of the lattice cell volumes between these two rutile oxides.

DOI: 10.1103/PhysRevB.77.014302 PACS number(s): 63.20.kp, 61.72.up, 75.50.Pp, 75.30.Hx

I. INTRODUCTION

Wide band-gap oxide semiconductors, such as rutiles TiO_2 and SnO_2, when doped with transition metal ions, show a ferromagnetic (FM) magnetization at room temperature, a property interesting from the spintronics application viewpoint and puzzling scientifically.[1–5] The origin of the FM order at room temperature is controversial since it is connected with both the impurity dopant distribution and the parental structure defects (PSD), the interactions, and associations between them.

A dilute magnetic impurity dopant (ID) adopts in dilute magnetic semiconductors (DMS) a variety of distinct magnetic states appearing to underlie a common material property, which manifests itself as the magnetic inhomogeneity[5] (MIH) of the DMS. The origin of this inhomogeneity could be deeply related to the mechanism of magnetic exchange (ME) yet undetermined. Nonisoelectronic substitution may result in a conductivity-related ME,[6] or create a distribution of static magnetic moments in the lattice. Depending on dynamic characteristics of the magnetic impurities, several vibrational modes tend to localize on the impurity dopants (ID). From this viewpoint, a study of vibrational density of states (VDOS) of magnetic impurities in a DMS could be an important method aimed to disentangle the nature of MIH.

In this work, we determine the partial (^{57}Fe) VDOS of the local iron ID probe incorporated into the rutile phases of SnO_2 and TiO_2. Both powder and thin films were investigated and showed different VDOS, depending on synthesis conditions. The nuclear inelastic scattering (NIS) data turn to be quite useful in attaining a better understanding of the structural and chemical states of the diluted or clustered ID.

II. EXPERIMENT

Powders of $Sn_{0.9}Fe_{0.1}O_2$ were synthesized using the standard sol-gel route. The final annealing in air at ambient pressure was done at 600 °C. More details on the sample processing can be found elsewhere.[7]

Titanium dioxide films with ca. 100 nm in thickness were prepared on sapphire substrates using the pulsed laser deposition (PLD) technique from the sintered at 1200 °C target of 94 w/w % TiO_2 and 6 w/w % Fe_2O_3. The film properties changed depending on the substrate temperature and gas pressure. In this work, the temperature of substrate was chosen to be kept constant (650 °C) and a series of films deposited onto *R* cuts of sapphire substrates at different pressures was studied.

The films were characterized by x-ray diffraction, conversion electron Mössbauer spectroscopy (CEMS) and x-ray absorption fine structure (XAFS).[7–9] In the Θ-2Θ x-ray diffraction patterns, the rutile Bragg reflections (101), (202), and (303) were observed additionally to the substrate peaks. Corresponding rutile rocking curves broaden as the deposition pressure increases [Fig. 1(a)].

Grazing incidence scattering geometry was employed for NIS experiments on thin film and powder samples [Figs. 1(b) and 1(c)]. The Spring-8 storage ring was running in the special NIS timing mode "11-bunch train × 29" with the bunch interval of 145.5 ns. Nested asymmetric Si(511) and Si(975) channel cut monochromator at the beamline BL09XU provided the bandwidth (FWHM) of 2.5 meV. X-ray fluorescence FeK_α(6.4 keV) excited via conversion channel was the dominant delayed scattering. An assembly of fast silicon avalanche detectors (APD) has allowed collecting the intensity scattered into large solid angle. The NIS spectra were recorded by detuning the energy band within ±80 meV around the resonant energy E_r=14.4125 keV. The ^{57}Fe nuclear transition was excited via creating/annihilating phonons, a phenomenon complementary to Mössbauer effect. This NIS spectral range ($\pm 0.555 \times 10^{-5} E_r$ around E_r) was 10^5 times broader compared to the typical range of magnetically split high-spin $^{57}Fe^{3+}$ Mössbauer spectra (MS).

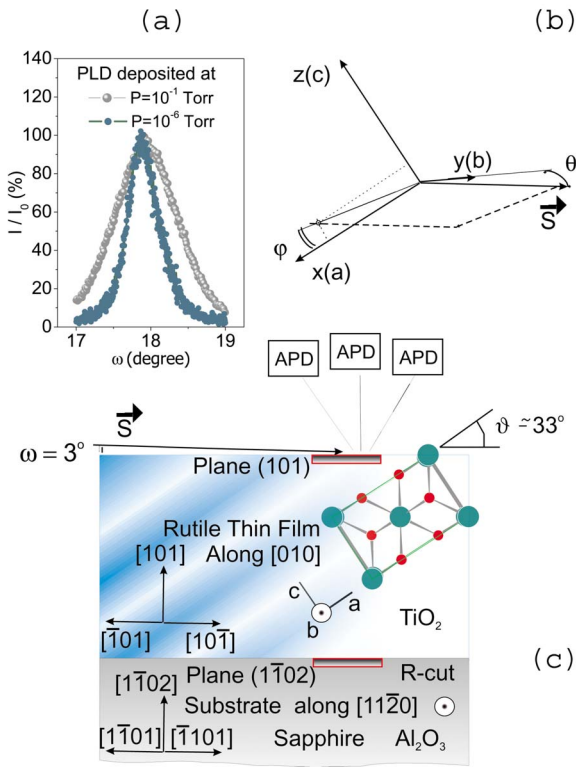

FIG. 1. (Color online) Characterization of the structure of TiO_2 films, geometry of scattering experiments, and film-substrate epitaxial relationship. In (a), the out-of-plane ω-rocking curves of the (101) reflection for the films deposited at the pressures of 10^{-1} Torr and 10^{-6} Torr exhibit the FWHM of 1° and 0.5°, respectively. (b) Spherical coordinate system represents the general orientation of the grazing incidence radiation wave vector $\vec{s}$ in the frame of rutile lattice axes as described by the zenith angle Θ and azimuth angle φ. In (c), the film is oriented at $\Theta=90°$, i.e., $\vec{s}_{\perp}[010]$; in this orientation, the structure of epitaxial film is shown projected onto the rutile plane (010).

III. RESULTS

In Fig. 2, the vibrational DOS determined from the NIS spectra for $Sn_{0.9}Fe_{0.1}O_2$ powder is shown. We compare the modes of ^{57}Fe ID with the native modes of Sn in SnO_2, as determined from the NIS spectra of the Mössbauer isotope ^{119}Sn, published previously.[10] The mass ratio of iron to tin is only 0.53, however, one sees in Fig. 2 that iron probes faithfully the tin site. The shape of the VDOS of ^{57}Fe probe in the polycrystalline "mixed crystal" $Sn_{0.9}Fe_{0.1}O_2$ closely follows the shape of VDOS of the native species Sn in the parent rutile SnO_2. In agreement with the lighter mass of Fe, its spectrum upon the whole is harder than the spectrum of Sn is SnO_2, and the best fit between the centers of gravity of two DOS can be obtained by rescaling the energy axis with the factor of 1.07 [keeping unchanged the area under DOS, Fig. 2(b)].

Force constant change is another ID effect expected in $Sn_{0.9}Fe_{0.1}O_2$ to appear concomitantly with the mass defect. The nearest-neighbor (NN) force constant change Δf is a well known effect of nonisoelectronic substitution, e.g., in III-V superconductors, where the changes $\Delta f>0$ and $\Delta f<0$ appears for charged donors and acceptors, respectively.[11] In both cases of electron and hole donors the significant magnitude $|\Delta f/f|$ of ca. 25% was observed and attributed to Coulombic interaction between charged impurity and its nearest neighbors.[11] The fact the Fe^{3+} hole donor probes immediately the partial DOS of Sn^{4+} might be explained by the almost complete cancellation of mass defect and force constant changes, with the residual VDOS shift of eventually less than 7% only.

The local modes of lighter mass ID should appear above certain threshold of mass ratio.[12] When the mass of ID is twice as little as the mass of the host, the local modes are predicted at the frequencies ca. 10% larger than upper cutoff frequencies of the host. In Fig. 2 we do not observe any local mode as a separate line split off from the rest of the DOS. Softening of spring constants of the Fe^{3+} hole donor explains as well the missing local mode of Fe^{3+} in SnO_2.

When Fe^{3+} substitutes Sn^{4+} in $Sn_{0.9}Fe_{0.1}O_2$, the octahedral environment of the ID may be varied if the oxygen vacancies are introduced into the first coordination sphere of Fe^{3+}. Clearly, the charge difference between Fe^{3+} and Sn^{4+} has not necessarily to be compensated by 5% of vacancies distributed in the midst of the oxygen sublattice, but could be also balanced by a much smaller amount of the interstitials of Sn^{4+} or Sn^{2+}, supposed to be the main PSD,[13] underlying lattice pointlike disorder in rutile SnO_2. We conclude that iron is well dilute in the host lattice of SnO_2 powders and it probes faithfully the vibrations of Sn^{4+} in its octahedral environment of the rutile structure.

The MS of these SnO_2 powders showed only paramagnetic iron at room temperature, although FM behavior was observed in magnetization.[7] These results are therefore indicative of dilute ferromagnetism incipient in the DMS based on SnO_2.

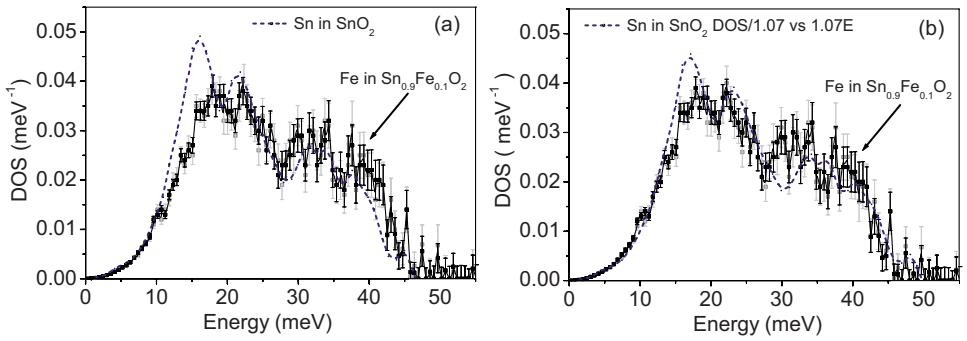

FIG. 2. (Color online) (a) Partial vibrational DOS of ^{57}Fe in $Sn_{0.9}Fe_{0.1}O_2$ powder compared to original and (b) rescaled by factor 1.07 partial VDOS of ^{119}Sn in SnO_2.

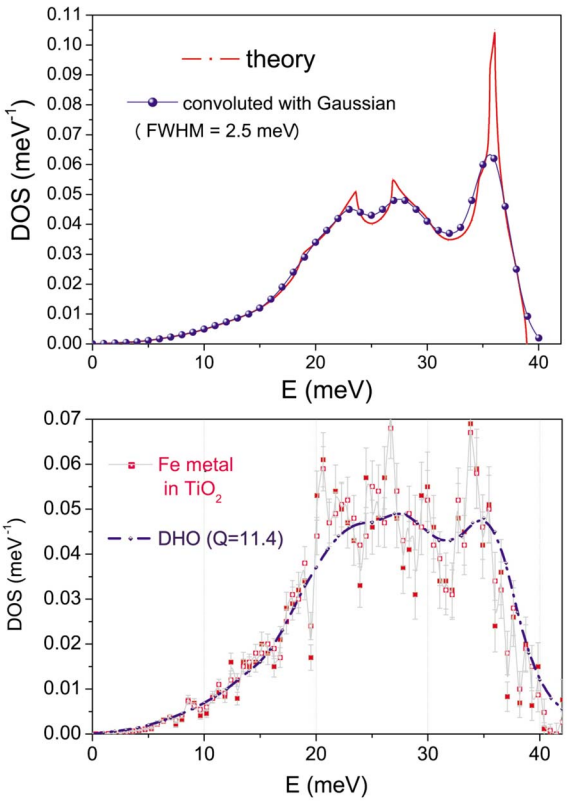

FIG. 3. (Color online) VDOS of α-Fe calculated from the fifth-neighbor general force constant model $g(E)$ (Ref. 14), its convolution with the resolution-limiting Gaussian [Eq. (6)] and $G(E)$ for quality factor $Q=11.4$ in Eq. (1), fitted to the experimental partial ^{57}Fe DOS of TiO_2 DMS PLD thin films deposited at 10^{-8} Torr.

According to CEMS[8] and XAFS,[9] the series of films of Fe-doped TiO_2 deposited in the high-vacuum and low-vacuum conditions in the range of oxygen pressures from 10^{-1} to 10^{-8} Torr using targets of $Ti_{0.94}Fe_{0.06}O_2$ are characterized by the variety of different Fe chemical states, which are dramatically influenced by the value of residual oxygen pressure. We start the discussion of vibrational properties of ^{57}Fe in this series from the films, which were prepared in high vacuum. Some of the films were then postannealed in air at 300 °C, however, such low-temperature annealing did not vary much the MS,[8] and we observe no significant changes in their DOS after the postannealing. Shown in the bottom right panel of Fig. 3 is the DOS of ^{57}Fe in the as-prepared at 10^{-8} Torr film of $Ti_{0.94}Fe_{0.06}O_2$.

Chemical shifts in XAFS and MS and the experimental DOS in Fig. 3 are indicative of metallic state of iron, therefore, we compare our result with the DOS of bulk α-Fe. The energy range of our DOS is limited by 40 meV, and its shape resembles to the DOS of metallic Fe, however, broadened. Two origins of the broadening of the spectral features are examined in Fig. 3. First, the theoretical DOS predicted in Ref. 14 must, prior to comparison with experiment, be slightly broadened by virtue of finite energy resolution of our high-resolution monochromator. The standard convolution of the bulk α-Fe DOS with Gaussian ($\sigma=1.06$ meV, FWHM $=2.5$ meV) affects most strongly the narrow DOS peak originating from longitudinal phonon branch at zone edge. Since the van Hove singularity peak at 36 meV is suppressed more strongly in the experimental DOS than in the Gaussian-convoluted DOS of the bulk α-Fe, it is tempting to look for an additional source of broadening. It appears that an additional broadening of spectral features may result from the finite size of small clusters, in which the phonons lifetime is shortened.[15,16] Using the model of damped harmonic oscillator (DHO) for a small cluster, prior to convoluting the result with Gaussian, the bulk Fe DOS (Ref. 14) $g(E)$ was integrated:

$$G(E) = \int_0^\infty D(E,\varepsilon) g(\varepsilon) d\varepsilon \tag{1}$$

with the DHO profile:[17]

$$D(E,\varepsilon) = \frac{2}{\pi Q E}\left[\left(\frac{E}{\varepsilon} - \frac{\varepsilon}{E}\right)^2 + \frac{1}{Q^2}\right]^{-1}. \tag{2}$$

It is presumed in Eq. (2) that the width of each vibrational state of DOS depends only on the energy of this state. Moreover, it is supposed that the phonon linewidth Γ is linear with phonon energy. Equation (2) is thus obtained via substituting $\Gamma(\varepsilon)=\varepsilon/Q$ into the well-known expression for the DHO line shape:

$$D(E_Q,\varepsilon) = \frac{2}{\pi}\frac{\varepsilon E_Q \Gamma(\varepsilon)}{(\varepsilon^2 - E_Q^2)^2 + E_Q^2 \Gamma^2(\varepsilon)}. \tag{3}$$

The meaning of "Q" is different in Eqs. (2) and (3). In Eq. (2) it means the DHO quality factor, but in Eq. (3) it refers to the magnitude of momentum transfer that could be quoted as the "quota of phonon wavelength within one lattice cell." In order to estimate the phonon lifetime τ in a small iron cluster, we rewrite Eq. (3) as the combination of two Lorentzians,

$$D(E_Q,\varepsilon) = \frac{E_Q}{\sqrt{E_Q^2 - \Gamma^2/4}}\frac{\Gamma}{2\pi}\left[\left(\left(\varepsilon - \sqrt{E_Q^2 - \frac{\Gamma^2}{4}}\right)^2 + \frac{\Gamma^2}{4}\right)^{-1} - \left(\left(\varepsilon + \sqrt{E_Q^2 - \frac{\Gamma^2}{4}}\right)^2 + \frac{\Gamma^2}{4}\right)^{-1}\right] \tag{4}$$

so that in the limit of small asymmetry introduced into $D(E_Q,\varepsilon)$ by the second Lorentzian from full Lorentzian width at half maximum[18] $\Gamma \equiv \Gamma(\varepsilon)$ the phonon decay time τ can be estimated as follows:

$$\tau = \frac{2\hbar}{\Gamma(\varepsilon)}. \tag{5}$$

Our result $Q=11.4$ obtained through the least-squares fitting the experimental DOS (Ref. 19) with the resolution-broadened function

$$G_\sigma(E_Q) = \frac{1}{\sqrt{2\pi}\cdot\sigma}\int_0^\infty G(\varepsilon)\exp\left(-\frac{(\varepsilon - E_Q)^2}{2\sigma^2}\right)d\varepsilon \tag{6}$$

leads to the linewidth of 3 meV and to the decay time $\tau=0.44$ ps at the energy of 34 meV. From these data the size of the iron cluster can be derived. Here we use the estimation

TABLE I. Fitted values of the quality factor Q for a series of the energy rescaling factors α in Eq. (1). The theoretical expression for DOS in nanoclusters $G_\sigma(E_Q)$, see Eq. (6), was fitted with several fixed values of α to experimental DOS of Fe in TiO_2 films prepared in high vacuum (10^{-8} Torr).

α	0.94	0.95	0.955	0.96	0.965	0.97	0.975	0.98	0.99	1.00
Q	15.5	17.4	20.7	22.0	23.7	20.8	19.1	18.1	15.2	11.4

technique adapted previously for ball-milled nanocrystalline iron.[20] We suppose therefore that the spherical cluster diameter D_c is bigger by half than the travel distance between two points at its surface. Such a travel distance can be found as $v\tau$, taking the value of 2500 m/s for the group velocity v of phonons propagating along ⟨100⟩ direction of the bcc lattice of α-Fe around E_Q=30 meV. We obtain thus the travel distance of 1.2 nm and the cluster size of 1.9 nm. Our clusters with such a mean size are much smaller than the grains obtained through ball milling[20] or via inert gas condensation (IGC).[21] In the latter work, the NIS spectra measurements were done with a very good energy resolution of 0.6 meV. We estimated that in the NIS spectra, measured with such a high resolution, the Q values below ca. 50 are the primary factor of broadening near E_Q=30 meV. In our spectra, however, the energy resolution was four times worse than in Refs. 20 and 21, so that the resolution effect is quite comparable in magnitude with the effect of finite Q.

The most striking result, which in nanocrystalline Fe was not reported previously,[20–22] is the overall softening of DOS, including the zone edge regions. In Fig. 3, the experimental DOS is upon the whole softer than the theoretical function, obtained from Eq. (6) via single-parametric fit of the Q factor. The high-energy cutoff edge in the fitted function is by a few meV harder than the cutoff of the experimental DOS. In addition, it is clear in Fig. 3 that the fitted function is rather structureless compared to experimental DOS, although the statistical noise somewhat shadows this effect.

Therefore, in the next step, we modified the least-square fit function by introducing the additional parameter α scaling the energy of theoretical DOS. Here, instead of Eq. (1), Eq. (7) was used to substitute the function $G(E)$ into Eq. (6):

$$G(E) = \int_0^\infty D(E,\varepsilon) g(\alpha\varepsilon) d\varepsilon. \tag{7}$$

It is not straightforward to fulfill the two-parametric least square fitting when one of the parameters scales the argument ε; therefore, the single-parametric fitting was repeated for the series of 10 fixed values of α near 1. Both the quality of fit and the fitted Q value culminate at α=0.965 (Table I). Maximum Q at this softening of 3.5% is two-times larger than Q for α=1; therefore, if we suppose that the embedment of Fe clusters into TiO_2 matrix dilates them, then the cluster size approaches 4 nm, comparable to IGC iron.[21] From the pressure derivative of phonon energies for Fe nanocrystals[22] $E^{-1}dE/dP \approx 0.6\%/\text{GPa}$ we can estimate the negative "chemical pressure" of 5 GPa. The Fe metal segregation away from TiO_2 matrix may as well result in formation of

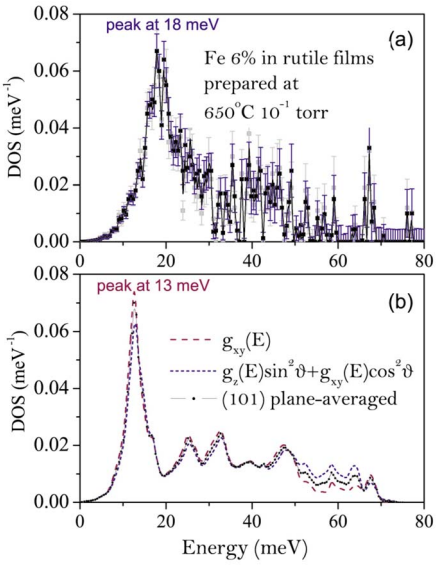

FIG. 4. (Color online) (a) Partial DOS of ^{57}Fe impurity in the pulsed-laser-deposited film of rutile TiO_2 prepared at the oxygen pressure of 10^{-1} Torr in comparison with (b) the intrinsic Ti direction-projected and plane-projected Ti DOS. The direction-projected DOS are calculated for the in-plane directions [0 1 0] $g(E)=g_{xy}(E)$ and [10 $\bar{1}$] $g(E)=\frac{1}{2}g_{xy}(E)\cos^2\vartheta+\frac{1}{2}g_z(E)\sin^2\vartheta$. The (101)-plane-projected DOS is the plane-averaged $g_{(101)}(E)=\frac{1}{2}g_{xy}(E)(1+\cos^2\vartheta)+\frac{1}{2}g_z(E)\sin^2\vartheta$. According to Ref. 27, the areas under each of the PDOS curves in (a) and (b) are normalized to unity; cf. a different way of the area normalization adopted for g_{xy} and g_z in calculations (Ref. 26): $\int g_{xy}(E)dE=2/3$ and $\int g_z(E)dE=1/3$.

clusters or thin layers of fcc γ iron, similarly to γ-Fe precipitation in bulk fcc metals[23] and γ-Fe pseudomorphic growth on surfaces of fcc metals.[24] Since the DOS of the fcc γ-Fe is somewhat softer[23] than the DOS of the bcc α-Fe, the idea of γ-Fe allows explaining alternatively (without chemical pressure effect) the general DOS softening observed in our experiment. Some "ambiguous" Mössbauer components with reduced (compared to α-Fe) hyperfine fields were reported previously,[8] however, it is not clear at present whether their $H_{hf} \cong 30$ T suits the range of variability of H_{hf} in γ-Fe at room temperature.

DOS in TiO_2 films deposited in raw vacuum at P (O_2) of 10^{-1} Torr is very different from the DOS of clustered iron. These films were characterized in CEMS data[8] by the quadrupole doublet with the splitting of 0.93 mm/s and chemical shift of 0.37 mm/s, characteristic of the Fe^{3+} ions in a paramagnetic state. The shift of Fe K-edge in XANES data[7] is also indicative of the Fe (III) diluted in the TiO_2. The Fe^{3+} ions are supposed to occupy the Ti site, therefore, in Fig. 4, we compare the partial DOS of ^{57}Fe in the low-vacuum-deposited films with the partial contribution of Ti into the phonon DOS of TiO_2.

Generalized phonon DOS of TiO_2 involving contributions of both Ti and O atoms was experimentally determined using inelastic scattering of neutron.[25] These vibrations occupy the region up to 100 meV, much broader than observed in Fig. 4.

However, a recent *ab initio* calculation in local density approximation (LDA) of lattice dynamics in TiO_2 has showed[26] that the modes with large weight of Ti vibrations are bunched only at frequencies below 17 THz ($E \sim 70$ meV). Calculated in Ref. 26 were also the Ti DOS anisotropic contributions, which enable as well the comparison with experiments on single-crystalline samples. The theoretical treatment due to Kohn, Chumakov, and Rüffer[27] allows one to derive the phonon projected densities of states (PDOS), whenever the appropriately collected anisotropic NIS spectra are available. Our thin films of $Ti_{0.94}Fe_{0.06}O_2$ on sapphire showed in x-ray diffraction patterns only the (101) reflections, indicating their single-crystalline nature. In our NIS experiments, the grazing incidence angle was fixed near 3° [Fig. 1(c)], however, no special care was taken to set up the film with a fixed in-plane orientation with respect to the incident beam. While the film and incident beam were both locked near the horizontal plane, no clear observation of the angular dependence of DOS was made, although in several experiments the films were rotated arbitrarily around the vertical axis. We show in Fig. 4(a) that, despite there exist in rutile a significant vibrational anisotropy,[26] only smaller variations of the DOS depending on the in-plane orientation are expected.

Due to tetragonal symmetry of rutile the complete set of PDOS consist of $g_z(E)$ and $g_{xy}(E)$ with $g_{xy}(E) \equiv g_x(E) = g_y(E)$. The alignments of the wave vector $\vec{s}$ parallel to either of mutually orthogonal directions in the plane of the film surface, [0 1 0] and [1 0 $\bar{1}$], are expected[27] to generate the nonequivalent NIS spectra. Since the (101) planes are the twinning planes of rutile structure, the TiO_2 rutile films on sapphire plane (1 $\bar{1}$ 0 2) appears to be twinned. Twinning allots a channel to relieve the significant interfacial lattice spacing mismatch from TiO_2 to Al_2O_3 of −3.6% along [0 1 0]||[1 1 $\bar{2}$ 0]and of 6.4% along [$\bar{1}$ 0 1]||[1 $\bar{1}$ 0 1]. Previously, the growth twin boundaries in the (101)-rutile films on sapphire were observed laying both parallel to film surface,[28] and in perpendicular direction.[29] Our film prepared at 10^{-1} Torr in Fig. 4 shows the largest FWHM of 1°, and no iron clusters were observed in this film. The large FWHM in such films was argued[28] to correlate with high density of twin boundaries perpendicular to the film normal direction. In our films, as the deposition pressure decreases, the rocking curve narrows. We found above that iron segregates into metallic clusters at the extremity of deposition pressure as low as 10^{-8} Torr. Thus, narrowing the rocking curves with lowering the deposition pressures should be attributed either to decreasing the twin density, or decreasing the strains from diluted Fe^{3+}, or to a combined effect. If the diluted impurity ions tend to decorate the dislocations, stacking faults or twin boundaries, the Fe precipitation into clusters may favor the defect release from TiO_2.

When the in-plane texture of a film is not clear, one can consider its average DOS obtained in a series of experiments as a plane-projected (or plane-averaged) DOS. Experimentally, the measurement of such a plane-projected DOS can be done using the grazing incidence scattering from a sample rotating around a vertical axis. In anisotropic single crystal of arbitrary orientation with respect to the incident beam [Fig. 1(b)] the general expression for DOS is

$$g(E) = g_x(E)\cos^2\alpha + g_y(E)\cos^2\beta + g_z(E)\cos^2\gamma. \quad (8)$$

Powder-averaging the directional cosines, e.g., in case of Fig. 2 where $g_x = g_y = g_{xy}$, gives

$$g(E) = \frac{2}{3}g_{xy}(E) + \frac{1}{3}g_z(E). \quad (9)$$

In our choice of coordinate system [Fig. 1(b)], $\cos\alpha$ and $\cos\gamma$ are expressed via the zenith angle Θ ($\equiv\beta$) and the azimuth angle φ as follows: $\cos\alpha = \sin\Theta\cos\varphi$; $\cos\gamma = \sin\Theta\sin\varphi$. A plane-averaged DOS $g_{(hkl)}(E)$ can be expressed through $g_x(E)$, $g_y(E)$, and $g_z(E)$:

$$g_{(hkl)}(E) = \frac{1}{2\pi}\int_0^{2\pi}\left[g_y(E)\cos^2\Theta + g_x(E)\sin^2\Theta\cos^2\varphi + g_z(E)\sin^2\Theta\sin^2\varphi\right]d\Theta. \quad (10)$$

Substituting for the azimuth angle φ the derived from rutile lattice parameter aspect ratio value $\vartheta = \arctan(c/a)$ we obtain the result of integration for our plane (101):

$$g_{(101)}(E) = \frac{1+\cos^2\vartheta}{2}g_{xy}(E) + \frac{\sin^2\vartheta}{2}g_z(E). \quad (11)$$

This result coincides with the average of two direction-projected DOS in the plane:

$$g_{[010]}(E) = g_{xy}(E),$$

$$g_{[10\bar{1}]}(E) = g_{xy}(E)\cos^2\vartheta + g_z(E)\sin^2\vartheta. \quad (12)$$

Incidentally, due to a specific aspect ratio in rutile, $g_{[10\bar{1}]}(E)$ is very similar to the powder-averaged DOS of rutile [Eq. (9)].

We observe in Fig. 4 that the DOS of ^{57}Fe in TiO_2 differs from zero in excess of the experimental error only below 50 or 55 meV. This is consistent with the heavier (by ca. 20%) mass of Fe with respect to Ti. However, the lowest peak of DOS at 13 meV, observed by neutron scattering[25] and attributed entirely[26] to the vibrations of Ti does not manifest itself in the spectra of ^{57}Fe. Instead, we observe the peak near 18 meV, i.e., at the energy, where the partial DOS of Ti show the minimum. This energy location of the ^{57}Fe impurity mode is somewhat resembling the energy location of gap modes.[12,30] Such impurity gap modes are localized; however, their mutual coupling at high level of impurity doping may lift the degeneracy of longitudinal and transverse localized vibration modes.[31] In pure TiO_2, the lowest in energy peak of Ti vibrations at 13 meV comes from the zone-edge singularity for the transverse acoustic (TA) phonons.[25] On the other hand, the dispersion curves in rutile[25,26,32] show that the longitudinal acoustic (LA) branches rise up to at least twice higher energy, where they are joined with the bottom of optic band. Thus, in fact, the rutile TiO_2 has no clear gap in the phonon DOS.

The impurity mode at 18 meV is located below the optic band of TiO_2, above TA phonon of TiO_2 and overlapped with the LA phonon of the matrix. Such an overlap may indicate on the resonant character of the impurity mode with respect to longitudinal motion. In semiconductors doped with impu-

rities of a heavier mass, and/or reduced force constant, the resonant bands are frequently formed by a group of modes which have large amplitudes near impurity.[12] These resonant bands are derived from the gap modes when the frequency of the gap mode drops below the top of acoustic band. In the case of ^{57}Fe in TiO_2, the resonant band around 18 meV is well separated from the TA phonon at 13 meV, therefore, the transverse motions should be quite well localized near the impurity, in a way similar to localization of the gap modes.[12,30]

IV. DISCUSSION

Comparing two rutiles, we see in spite of larger mass difference between the mass of impurity m_i and host cation m in SnO_2 than in TiO_2 that the difference between partial DOS of Fe and Ti is larger. The impurity DOS and host DOS relationships are qualitatively different between these two rutiles. The modes of ^{57}Fe ID probe faithfully the DOS of the host cation in SnO_2, but create the local or resonant excitation gaplike band in TiO_2. From the opposite signs of the mass defect $(m-m_i)/m$ in TiO_2 and SnO_2 one may expect that the mass defect and force constant changes are synergistic in TiO_2, as opposed to SnO_2, where they strongly extinguish each other.

The occurrence of local ID modes and gap modes is predicted already within a simple diatomic chain model, however, this model fails to predict the resonant modes evolving from the gap modes when the ID mass m_i is sufficiently large. Weakening the force constant of bonds linking the ID with its nearest neighbors f_i as compared to the host force constant f_h permits to infer the resonant bands.[12] More appropriate model in rutile may include as adjustable parameters two different forces, those between nearest neighbors, f_{MO}, and those linking anions f_{OO}. Such model sophistication would be coherent with the close packing of oxygens in rutile, whose oxygen sublattice can be considered as slightly distorted hexagonal close packed (hcp) structure.[33] Furthermore, the occurrence in hcp-related rutile structure of the special quasihexagonal axis doubles the number of force parameters. It lifts the bond degeneracy among six bonds in the MO_6 octahedron. There appears a nonequivalence between four bonds with nearest-neighbor (NN) forces K'_{MO} and two bonds with nearest-neighbor forces K_{MO}. Moreover, among 12 next-nearest-neighbors of an anion in the hcp lattice, there appears due to distortion eight NN connected with forces K'_{OO} and 4 NN connected with forces K_{OO}.[34]

The values of four sorts of force constants K'_{MO}, K_{MO}, K'_{OO}, and K_{OO} were calculated[34] in both rutiles TiO_2 and SnO_2. In TiO_2, they are 88, 78, 55, and 94 N/m, respectively, and in SnO_2, they are 149, 146, 48, and 40 N/m, respectively.[34] The latter result shows in SnO_2 that the nearest-neighbor interactions of an anion are ca. three times stronger than the next-nearest-neighbor (NNN) interactions. It is not so in TiO_2, where NN and NNN springs are of comparable strengths. Oxygens are thus much more closely packed in TiO_2 than in SnO_2 due to ca. 10% difference of the lattice cell volumes between these two rutile oxides.

It was emphasized by the author[34] that the rigidity of the O-O interaction is an important factor in TiO_2. Therefore, when K'_{MO} and K_{MO} are weakened around the hole donor Fe^{3+}, due to Coulombic interaction between charged impurity and its neighbors,[11] the rigidity in TiO_2 is maintained by the strong forces K'_{OO} and K_{OO}. With the reduced strength of its NN interactions the Fe ID should be rattling in a rigid cavity at a frequency strongly reduced compared to the frequency of optic phonons in TiO_2. The energy of such a motion turns out to be close to the energy of lowest-lying sharp DOS peak from octahedral Fe in typical Fe-based complex close-packed oxides, such as spinels.[35] The local mode is centered at the impurity atom, that is, its maximum displacement amplitude is at ^{57}Fe ID, in contrast to original optic phonon modes of TiO_2, which are contributed by much larger displacement eigenvectors for O than for Ti.

In contrast, the case of SnO_2 shows that Fe could be a faithful probe for the partial DOS of some cations in oxides, and the shape of impurity DOS roughly follows the shape of the DOS of host cations. In agreement with previous LDA study[13] of electronic structure in SnO_2 we find that the oxygen vacancies are probably not the single defects accommodated by structure, because the oxygen vacancies in large number (5%) are expected to modify strongly the first coordination sphere of Fe^{3+}. The plausible explanation[13] of attractive interactions between an oxygen vacancy and tin interstitial is also supported by the observation[36] of a too high for Fe^{3+} MS chemical shift (δ=0.47 mm/s relative to α-Fe) for low doping levels (x=0.005 in $Sn_{1-x}{}^{57}Fe_xO_2$). According to Ref. 13, in pure SnO_2, both tin interstitial and oxygen vacancy donate electrons into conductivity band due to a bound state formed of these two defects. These electrons are sensed at very small x via increased value of δ, but when x increases δ takes the ordinary value of 0.37 mm/s. There occurs the localization of electrons with Fe doping and a formation of electronic molecules[37] is a plausible model since the oxidation states in a host lattice site are rather Sn^{4+} and Sn^{2+} than Sn^{3+}. According to this model,[37] we have determined the "phonon cloud," more exactly just the partial contribution of ^{57}Fe into it, capable to trap a few electrons into a stringlike or planar configuration and create a stable or metastable cluster of electrons. Interestingly, the electrons trapped into the electron cluster could mediate the superconducting coupling among itinerant carriers in high-T_c superconductors[38] via exchange by their high-frequency electronic intramolecular vibrational modes, termed vibrons. Magnetic exchange among localized moments could be another consequence of the high-frequency vibronic states in thus created electronic molecules. Planar configurations of the electronic molecules in thin films may therefore explain the strong anisotropy of the persistent currents,[39] observed via anisotropy of FM magnetization.

Previously, in the rutile $Sn_{0.95}Fe_{0.05}O_2$, Fitzgerald *et al.*[40] and Coey *et al.*[41] observed the T_c values of 360 K and 610 K in a ceramic target and in the PLD film made of it, respectively. These values of T_c were understood as depending on the amount of iron ID incorporated into the DMS matrix. Although in the film all the iron ID permeated into SnO_2 form almost random ID distribution and raise the T_c value of the DMS matrix up to 610 K, the film shows MIH in MS with the majority of ID (77%) in paramagnetic state.[41] Such a MIH is explained within the polaronic theoretical picture of

DMS.[5,41] However, Sakuma *et al.*[7] found a fully paramagnetic MS of iron (III) ID in several samples of $Sn_{0.9}Fe_{0.1}O_2$ showing significant FM magnetization at room temperature. This may imply a dynamic nature of MIH.

A coexistence of a paramagnetic doublet and a magnetically split component in MS can be thought to result from superparamagnetic (SPM) relaxation supposed the magnetic clusters are having a broad distribution in size. In DMS, two distinct kinds of SPM behavior are usually observed. First, it is an intrinsic behavior of magnetic ions distributed not quite randomly in the parental lattice of the host DMS.[42] Second, an extrinsic SPM behavior of the metallic Co nanoclusters segregated away from $Ti_{1-x}Co_xO_{2-\delta}$ was also previously observed.[43] Since the double-exchange-like (DEL) mechanisms of ME underlying the FM ordering in DMS were widely suggested,[6,44–46] the SPM behavior could be another common feature among DMS and manganites. Indeed, in classical DEL systems,[47] the appearance of SPM relaxation near T_c was postulated to explain the MS,[48] and some kind of relaxational behavior was suggested in two recent works on MS spectroscopy in Fe-doped DMS of ZnO (Ref. 49) and TiO_2.[50]

Alternative mechanisms of magnetic interactions among the ID and PSD are the magnetic exchange (ME) by a single charge carrier or via superexchange.[5,51,52] In many semiconductors and in dielectrics, it is a predictable situation that the nonisoelectronic substitution results in creation of defects of multiple sorts simultaneously. They are discernable by the distribution of compensating charge around the ID. The ID associations either with PSD or with trapped electrons or holes maintain the charge neutrality. The multiple ID environments and their nonuniform distribution make it possible for several alternative ME mechanisms to coexist, therefore, the issue is in uncovering the prevailing ME type, ensuring the highest value of T_c.

The vibrational NIS spectroscopy has a greater potential of unveiling the local mode signatures of ID multiple-site DMS due to development of site-selective technique.[53] In this technique, from time-delay spectra of the scattered radiation the magnetic properties of multiple sites are discerned according to their vibrational frequencies. Magnetic and quadrupolar hyperfine energies can be extracted from quantum beats in time-delay spectra. Fourier spectroscopy of quantum beatings[54] allows a better accuracy in determining the hyperfine parameters than the resolution-limited accuracy of conventional Mössbauer spectroscopy. In this work, however, we confined ourselves to the ordinary NIS technique, whilst no records of time spectra were performed. We believe that, if multiple Fe ID sites in our samples are present with a significant abundance, no large differences occur between their vibrational spectra, at least in SnO_2. This is because the net total spectrum of ^{57}Fe in $Sn_{0.9}Fe_{0.1}O_2$ is close to the spectrum of Sn in SnO_2.

Finally, it is worth to discuss the aptitude of vibrational spectroscopy with nuclear ^{57}Fe ID probe to affirm the intrinsic or extrinsic nature of the high-T_c magnetic order. In Co-doped anatase TiO_2 thin films, the examples of extrinsic FM order were already known, as established, e.g., from the line shape of the magnetic circular dichroism spectra.[43,55] In one work, the high T_c FM ordering was attributed entirely to clustered Co metal.[55] Another work in the anatase PLD thin films showed the value of T_c as nearly high as T_c of bulk Co metal (1180 K); the Co clustering was seen in scanning transmission electron microscope and in spectra of electron energy loss.[43] However, the authors[43] found that the distribution of residual diluted Co in the rutile lattice are also a source of FM ordering at T_c of 650 K, in its turn, intrinsic. Such a diversity of the origins of multiple values of FM T_c in the same sample shows clearly the importance of bearing in mind a distribution of multiple charge and magnetic states of the ID species, detectable at small doping levels exclusively by local impurity-selective techniques.

V. CONCLUDING REMARKS

The vibrational properties of the nuclear probe ^{57}Fe substituted into cationic site of the rutile oxides have demonstrated a large difference between TiO_2 and SnO_2. The relationships between the vibrational densities of states of the host and impurity cations are qualitatively different between these two rutiles. In SnO_2, the impurity and host vibrational bands just about coincide in energy, while in TiO_2 the majority of impurity modes are grouped in the minimum of the host cationic DOS. Such the difference between the gaplike impurity modes in TiO_2, and the only slightly perturbed crystalline hostlike modes in SnO_2 was found to be consistent with four-force-constant model prediction. These two examples demonstrate that the vibrational probe could be effective at both local and long-range scales. The magnetic inhomogeneity commonly observed in DMS materials could be dynamic in its nature, therefore, we showed how the studies of the local modes of magnetic impurities and interactions between them opens the way to revealing the origin of the high-T_c magnetism.

The synthesis of powder in air or the pulsed-laser-deposition of thin films in dynamic vacuum results in dilution of iron in SnO_2 and in TiO_2. However, the NIS spectra measurements prove without ambiguity the existence of metallic Fe clusters when they are formed in high-vacuum (10^{-8} Torr) deposited films of TiO_2. The metal cluster size of 4 nm was estimated from the phonon lifetime except, however, the phonon line broadening due to phonon confinement the overall DOS softening was observed caused most probably by the cluster embedment inside the oxide matrix.

ACKNOWLEDGMENTS

The authors are indebted to T. Hasegawa for his encouragement and promotion of the work at the starting point of our investigation. This work was supported by Asahi Glass Foundation. A.I.R. acknowledges the additional financial support provided through RFBR Grant No. 07-02-91201. We also thank K. Inaba for preparation of the ^{57}Fe doped films.

*Corresponding author. FAX: +7-383-330-70-16; rykov@academ.org, rykov3@yahoo.com

[1] Y. Matsumoto, M. Murakami, T. Shono, T. Hasegawa, T. Fukumura, M. Kawasaki, P. Ahmet, T. Chikyow, S. Koshihara, and H. Koinuma, Science **291**, 854 (2001).

[2] P. Sharma, A. Gupta, K. V. Rao, F. J. Owens, R. Sharma, R. Ahuja, J. M. O. Gillen, B. Johasson, and G. A. Gehring, Nat. Mater. **2**, 673 (2003).

[3] S. B. Ogale, R. J. Choudhary, J. P. Buban, S. E. Lofland, S. R. Shinde, S. N. Kale, V. N. Kulkarni, J. Higgins, C. Lanci, J. R. Simpson, N. D. Browning, S. Das Sarma, H. D. Drew, R. L. Greene, and T. Venkatesan, Phys. Rev. Lett. **91**, 077205 (2003).

[4] K. Inaba, T. Hitosugi, Y. Hirose, Y. Furubayashi, G. Kinoda, Y. Yamamoto, T. W. Kim, H. Fujioka, T. Shimada, and T. Hasegawa, Jpn. J. Appl. Phys., Part 2 **45**, L114 (2006).

[5] J. M. D. Coey, M. Venkatesan, and C. B. Fitzgerald, Nat. Mater. **4**, 173 (2005).

[6] V. Fleurov, K. Kikoin, V. A. Ivanov, P. M. Krstajic, and F. M. Peeters, J. Magn. Magn. Mater. **272**, 1968 (2004).

[7] J. Sakuma, K. Nomura, C. Barrero, and M. Takeda, Thin Solid Films **515**, 8653 (2007).

[8] K. Nomura, K. Inaba, S. Iio, T. Hitosugi, T. Hasegawa, Y. Hirose, and Z. Homonnay, Hyperfine Interact. **168**, 1065 (2006).

[9] K. Nomura, H. Eba, K. Sakurai, A. Rykov, and T. Hasegava, Thin Solid Films **515**, 8649 (2007).

[10] M. Y. Hu, T. S. Toellner, W. Sturhahn, P. M. Hession, J. P. Sutter, and E. E. Alp, Nucl. Instrum. Methods Phys. Res. A **430**, 271 (1999).

[11] K. Laithwaite, R. C. Newman, and P. D. Greene, J. Phys. C **8**, L77 (1975).

[12] A. S. Barker and A. J. Sievers, Rev. Mod. Phys. **47** (Suppl.2), S1 (1975).

[13] C. Kilic and A. Zunger, Phys. Rev. Lett. **88**, 095501 (2002).

[14] V. J. Minkiewicz, G. Shirane, and R. Nathans, Phys. Rev. **162**, 528 (1967).

[15] B. Fultz, C. C. Ahn, E. E. Alp, W. Sturhahn, and T. S. Toellner, Phys. Rev. Lett. **79**, 937 (1997).

[16] R. Rohlsberger, J. Phys.: Condens. Matter **13**, 7659 (2001).

[17] Here factor of 2 was introduced in the numerator of Eq. (2) normalizing to unity the area under $D(E,\varepsilon)$. This makes a difference with the expression for $D(E,\varepsilon)$ used previously in Refs. 15 and 16.

[18] Γ is also a popular notation for half width at half maximum; see, e.g., another version of Eqs. (3) and (4) by M. Kenzelmann, R. A. Cowley, W. J. L. Buyers, R. Coldea, M. Enderle, and D. F. McMorrow, Phys. Rev. B **66**, 174412 (2002).

[19] For the details of the DOS calculation procedure, see A. I. Rykov, K. Nomura, Ts. Sawada, T. Mitsui, M. Seto, T. Tamegai, and M. Tokunaga, Phys. Rev. B **68**, 224401 (2003).

[20] E. Bonetti, L. Pasquini, E. Sampaolesi, A. Derui, and G. Cicognani, J. Appl. Phys. **88**, 4571 (2000).

[21] L. Pasquini, A. Barla, A. I. Chumakov, O. Leupold, R. Rüffer, A. Deriu, and E. Bonetti, Phys. Rev. B **66**, 073410 (2002).

[22] A. B. Papandrew, A. F. Yue, B. Fultz, I. Halevy, W. Sturhahn, T. S. Toellner, E. A. Alp, and H.-k. Mao, Phys. Rev. B **69**, 144301 (2004).

[23] Y. Tsunoda, Y. Kurimoto, M. Seto, S. Kitao, and Y. Yoda, Phys. Rev. B **66**, 214304 (2002).

[24] T. Tanaka, A. Tajima, R. Morizumi, C. Oshima, Y. Tsunoda, M. Seto, S. Kitao, and T. Mitsui, J. Phys. Soc. Jpn. **74**, 1762 (2005).

[25] J. G. Traylor, H. G. Smith, R. M. Nicklow, and M. K. Wilkinson, Phys. Rev. B **3**, 3457 (1971).

[26] R. Sikora, J. Phys. Chem. Solids **66**, 1069 (2005).

[27] V. G. Kohn, A. I. Chumakov, and R. Rüffer, Phys. Rev. B **58**, 8437 (1998).

[28] Y. Gao, S. Thevuthasan, D. E. McCready, and M. Engelhard, J. Cryst. Growth **212**, 178 (2000).

[29] J. Y. Huang, B. H. Park, D. Jan, X. Q. Pan, Y. T. Zhu, and Q. X. Jia, Philos. Mag. A **82**, 735 (2002).

[30] G. Lucovsky, M. H. Brodsky, and E. Burstein, Phys. Rev. B **2**, 3295 (1970).

[31] A. A. Maraduduin and J. Oitmaa, Solid State Commun. **7**, 1143 (1969).

[32] F. Gervais and W. Kress, Phys. Rev. B **28**, 2962 (1983).

[33] A. F. Wells, *Structural Inorganic Chemistry* (Clarendon Press, Oxford University Press, Oxford, England, 1986).

[34] V. Maroni, J. Phys. Chem. Solids **49**, 307 (1988).

[35] A. I. Rykov, K. Nomura, T. Misui, and M. Seto, Physica B **350**, 287 (2004).

[36] K. Nomura, C. Barrero, J. Sakuma, and M. Takeda, Czech. J. Phys. **56** (Suppl. E), 75 (2006).

[37] F. V. Kusmartsev, Contemp. Phys. **45**, 237 (2004).

[38] F. V. Kusmartsev, Europhys. Lett. **57**, 557 (2002).

[39] J. M. D. Coey, Solid State Sci. **7**, 660 (2005).

[40] C. B. Fitzgerald, M. Venkatesan, A. P. Douvalis, S. Huber, J. M. D. Coey, and T. Bakas, J. Appl. Phys. **95**, 7390 (2004).

[41] J. M. D. Coey, A. P. Douvalis, C. B. Fitzgerald, and M. Venkatesan, Appl. Phys. Lett. **84**, 1332 (2004).

[42] D. Magana, S. C. Perera, A. G. Harter, N. S. Dalal, and G. F. Strouse, J. Am. Chem. Soc. **128**, 2931 (2006).

[43] S. R. Shinde, S. B. Ogale, J. S. Higgins, H. Zheng, A. J. Millis, V. N. Kulkarni, R. Ramesh, R. L. Greene, and T. Venkatesan, Phys. Rev. Lett. **92**, 166601 (2004).

[44] P. Kacman, Semicond. Sci. Technol. **16**, R25 (2001).

[45] V. M. Pereira, J. M. B. Lopes dos Santos, E. V. Castro, and A. H. Castro-Neto, Phys. Rev. Lett. **93**, 147202 (2004).

[46] K. Kagami, M. Takahashi, C. Yasuda, and K. Kubo, Sci. Technol. Adv. Mater. **7**, 31 (2006).

[47] C. Zener, Phys. Rev. **82**, 403 (1951).

[48] V. Chechersky and A. Nath, Low Temp. Phys. **28**, 562 (2002).

[49] G. Y. Ahn, S.-I. Park, I.-B. Shim, and C. S. Kim, J. Magn. Magn. Mater. **282**, 166 (2004).

[50] P. Xiaoyan, J. Dongmei, L. Yan, and M. Xueming, J. Magn. Magn. Mater. **305**, 388 (2006).

[51] T. Dietl, H. Ohno, F. Matsukura, J. Cibert, and D. Ferrand, Science **287**, 1019 (2000).

[52] R. Skomski, J. Zhou, J. Zhang, and D. J. Sellmyer, J. Appl. Phys. **99**, 08D504 (2006); J. Appl. Phys. **272-276**, 1967 (2004).

[53] M. Seto, Sh. Kitao, Y. Kobayashi, R. Haruki, Y. Yoda, T. Mitsui, and T. Ishikawa, Phys. Rev. Lett. **91**, 185505 (2003).

[54] A. I. Rykov, I. A. Rykov, K. Nomura, and X. Zhang, Hyperfine Interact. **163**, 29 (2005).

[55] J.-Y. Kim, J.-H. Park, B.-G. Park, H.-J. Noh, S.-J. Oh, J. S. Yang, D.-H. Kim, S. D. Bu, T.-W. Noh, H.-J. Lin, H.-H. Hsieh, and C. T. Chen, Phys. Rev. Lett. **90**, 017401 (2003).